JMEPEG
DOI: 10.1007/s11665-011-9864-9

1059-9495/$19.00

Nitinol Fatigue: A Review of Microstructures and Mechanisms

A.R. Pelton

(Submitted June 18, 2010; in revised form January 28, 2011)

Microstructural analyses of thermal or mechanical fatigued Nitinol show remarkable similarities and are characterized by an increase in dislocation density with increasing number of cycles. Dislocation bands, which are thought to be due to the effects of moving martensite interfaces, align with the martensite lattice invariant plane. These microstructural effects result in modification of transformation temperatures, strain (under stress-control) and stress (under strain-control). Processing has a major effect on fatigue properties, whereby optimized thermomechanically treated microstructures provide more stable (and predictable) behavior than the annealed microstructures.

Keywords electron microscopy, fatigue, nitinol, superelasticity

1. Introduction

Nitinol possesses a unique combination of properties, including shape memory and superelasticity, which affords its utility in a broad range of engineering applications (Ref 1, 2). For a design engineer, the enticement of generating repetitive motion with perfect recovery has driven many exciting avenues of research and development. According to the theories of Nitinol martensitic transformation, a Bain (shape) strain is accompanied by a lattice invariant strain with low-energy twins (Ref 3, 4). It is therefore implied that repetitive temperature- or stress-induced martensitic transformations could provide infinite fatigue lives. Unfortunately, experience has shown that Nitinol devices may suffer from several forms of fatigue damage that range from component shape change to catastrophic fractures. The purpose of this article is to review the literature on thermal and mechanical transformation cycling with an emphasis on the effects on microstructure. Owing to the expansive nature of this topic, this article will start with thermal cycling, a mode that is not used in engineering applications, but is useful to monitor fatigue effects. Effects of mean strain and strain amplitude, characteristic of in vivo cardiac pulse pressures on endovascular Nitinol stents, will also be reviewed.

2. Thermal Fatigue

Thermal fatigue is defined as cycling through the transformation temperatures multiple times; in the simplest cases, there is no application of external stress or strain. Differential scanning calorimetry (DSC) is an elucidating method to monitor the changes in transformation temperature due to stress-free thermal cycling. Figure 1 illustrates the behavior of annealed (900 °C for 30 min) $Ni_{50.5}Ti_{49.5}$ upon cooling to −150 °C and subsequent heating to 120 °C repeated for 100 cycles (Ref 5). These results show that the transformation temperatures decrease with increasing thermal cycles in agreement with earlier studies (Ref 6, 7). Note that the martensite temperatures decrease by more than 24 °C and that the R-phase peak appears after a few cycles and then increases by over 20 °C after 100 cycles. Transmission electron microscopy (TEM) analysis (Ref 5) of these thermally cycled specimens showed that the dislocation density increased from $\sim 10^{10}$ m^{-2} as annealed to 5×10^{14} m^{-2} after 100 thermal cycles, consistent with the observations reported by Miyazaki et al. (Ref 7). Extensive TEM diffraction contrast experiments demonstrate that dislocations form with $\mathbf{b} = a\langle 100\rangle$ with $\{011\}$ slip planes, comparable to those observed in recent studies (Ref 8, 9). This slip system corresponds to the twinning shear direction and twin plane in martensite (Ref 3, 4). The dislocations adopt an interesting morphology that provides clues as regards their origin. Figure 2 illustrates dislocation shear loops with the same character in a given region after one thermal cycle. Note also the dark band of tangled dislocations that runs diagonally in the micrograph. These bands are parallel to the $(\overline{0.889}, \overline{0.404}, 0.215)_A$ lattice invariant plane and are thus parallel to the martensite-austenite interface. The observations of dislocation bands suggest that the moving martensite interfaces act as crystallographic "snowplows" that force the initial $\langle 100\rangle\{011\}$ shear loops to slip (and cross slip) and then become locked in the sessile bands at the interface plane. During subsequent transformation cycles, additional dislocation debris becomes more tangled, shorter, and more curved after multiple cycles. These dislocations further impede the motion of the martensite interface, thereby requiring a larger driving force, and consequently lower temperatures, to initiate transformation (Ref 5).

3. Mechanical Fatigue

The ability to predict fatigue behavior of Nitinol subjected to cyclic mechanical motion is critical for safety of Nitinol

This article is an invited paper selected from presentations at Shape Memory and Superelastic Technologies 2010, held May 16-20, 2010, in Pacific Grove, California, and has been expanded from the original presentation.

A.R. Pelton, NDC, 47533 Westinghouse Dr., Fremont, CA 94539. Contact e-mail: alan.pelton@nitinol.com.

Published online: 16 February 2011

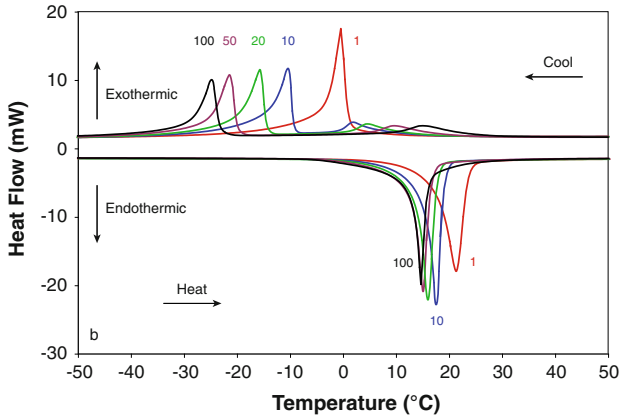

Fig. 1 DSC thermograms of heating and cooling cycles 1, 10, 20, 50, and 100 for annealed $Ni_{50.5}Ti_{49.5}$. The martensite and austenite peaks decrease in temperature whereas the R-phase transformation temperature increases with increasing numbers of cycles, according to Ref 5

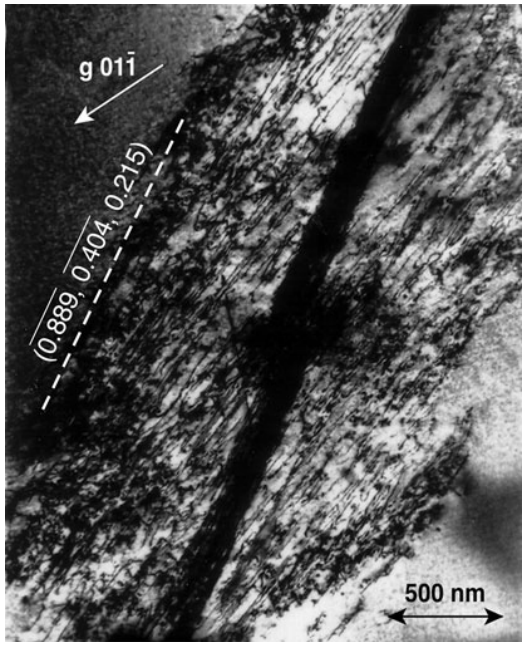

Fig. 2 Large array of dislocation loops in the cubic austenite phase of the $Ni_{50.5}Ti_{49.5}$ specimens after one thermal cycle that was imaged near $[111]_A$ with **g** $01\bar{1}$. Under these imaging conditions, the dislocation line directions, **u**, are parallel to $[020]_A$ and are perpendicular to the foil surface; hence the dislocations have a screw character. The strong-contrast dislocation band through the array is composed of mixed orientations and is parallel to $(0.889, 0.404, 0.215)$, according to Ref 5

biomedical devices. Nitinol fatigue investigations have yet to provide coherent insight into the mechanisms for all observed effects. Furthermore, early fatigue investigations suffered from three issues: First, the material was substandard in terms of modern practices (including homogeneity, purity, inclusion content, and thermomechanical processing). Therefore, the results from these investigations must be critically examined before application in a predictive model. Second, the early studies focused on materials that were tested in the annealed condition, which may lead to generalizations, but may not pertain to thermomechanically processed materials used for medical devices. Third, there are three basic approaches that have been used to evaluate the fatigue behavior of Nitinol: (1) stress-life, (2) strain-life, and (3) damage-tolerant analysis. Data obtained with one test method may not provide enough understanding of the results obtained from another test method.

Melton and Mercier (Ref 10) pioneered the field of Nitinol mechanical fatigue; no investigation before or since has attempted to understand behavior from all the three fatigue methods on the same Nitinol materials. Annealed binary compositions with A_f values between +10 to +110 °C were tested at room temperature in fully reversed uniaxial stress or strain amplitude. These investigations documented several important trends:

(1) Superelastic Nitinol provides longer lives and greater fatigue limits than thermal martensite subjected to stress-control fatigue. Melton and Mercier relate this observation to the difference in plateau strength between austenite and martensite. The 10^7-cycle stress fatigue limit is approximately 80% of the respective stress plateau (superelastic) or detwinning plateau (martensite).
(2) Repeated stress-controlled cycling leads to an increase in strain at constant stress amplitude. This implies that there is an accumulation of plasticity with cycling.
(3) The fatigue life of thermal martensite is superior to superelastic Nitinol under strain control. This observation may be due to the combined effects of a lower modulus and a reduced mechanical energy per cycle, which is related to the area of the stress-strain hysteresis loop.
(4) Repeated cycles under strain-control lead to cyclic hardening at constant strain amplitude. This hardening is speculated to be due to the effects of an increase in dislocation density with increasing cycles.

Nitinol medical implants present an entirely different deformation profile than those investigated by Melton and Mercier (Ref 10) and therefore require a different method to characterize the fatigue behavior. For example, Nitinol endovascular self-expanding stents may undergo a large single strain excursion (~10%) during constraint into a delivery system and then the opposite strain excursion during deployment into an artery (Ref 11, 12). Upon implantation, the stent is slightly oversized with respect to the vessel diameter; this "interference fit" produces a mean strain on the stent. Furthermore, the physiological movements from the cardiac systolic-diastolic cycle as well as musculoskeletal motions provide strain amplitudes. A TEM investigation was conducted on fatigued superelastic $Ni_{50.8}Ti_{49.2}$ specimens to understand the effects of processing and mean strain and strain amplitudes (Ref 13). Tensile specimens were machined from superelastic wire with a 3-mm-diameter gage. The specimens were either annealed at 900 °C for 30 min ($A_f = -15$ °C) or stress relieved at 500 °C for 10 min ($A_f = 20$ °C). Figure 3(a) shows the strain-controlled fatigue curves for the annealed specimen at 1.5% mean strain and 0.25% strain amplitude for 1, 10, and 100 cycles tested at room temperature. With increasing cycles, the hysteresis width decreases, the modulus increases, with both cyclic hardening and softening. The TEM microstructure after 10 cycles consists of banded austenite with a high density of dislocations ($\sim 10^{14}$ m^{-2}) with $\langle 100 \rangle / \{011\}$ slip systems interspersed with retained deformed martensite, Fig. 3(b). It is likely

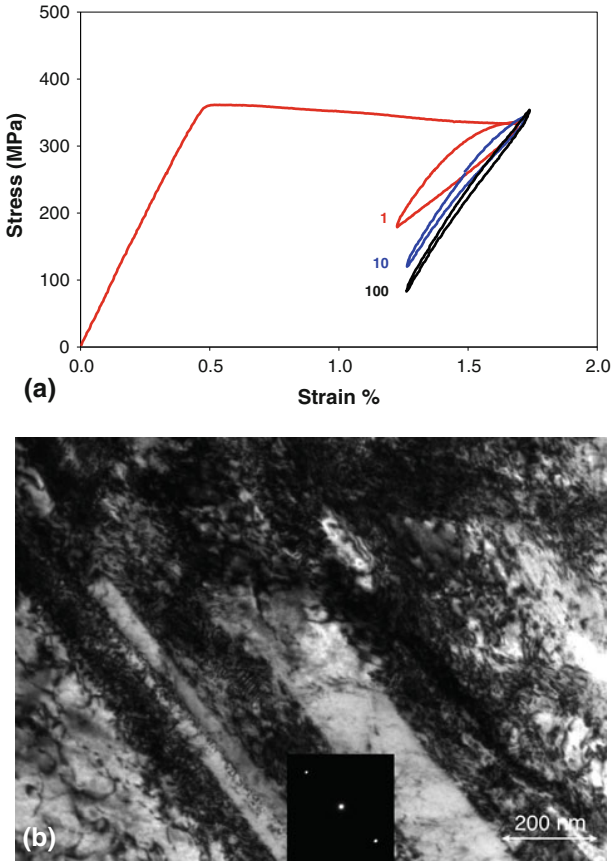

Fig. 3 (a) Stress-strain fatigue curves from annealed $Ni_{50.8}Ti_{49.2}$ under conditions of 1.5% mean strain and strain amplitude of 0.25%. Cycles 1, 10, and 100 are shown whereby the hysteresis width decreases, the modulus increases, with both cyclic hardening and softening with increasing cycles. (b) TEM microstructure after 10 cycles consists of banded austenite with a high density of dislocations ($\sim 10^{14}$ m^{-2}) with ⟨100⟩/{011} slip systems interspersed with retained deformed martensite, according to Ref 13

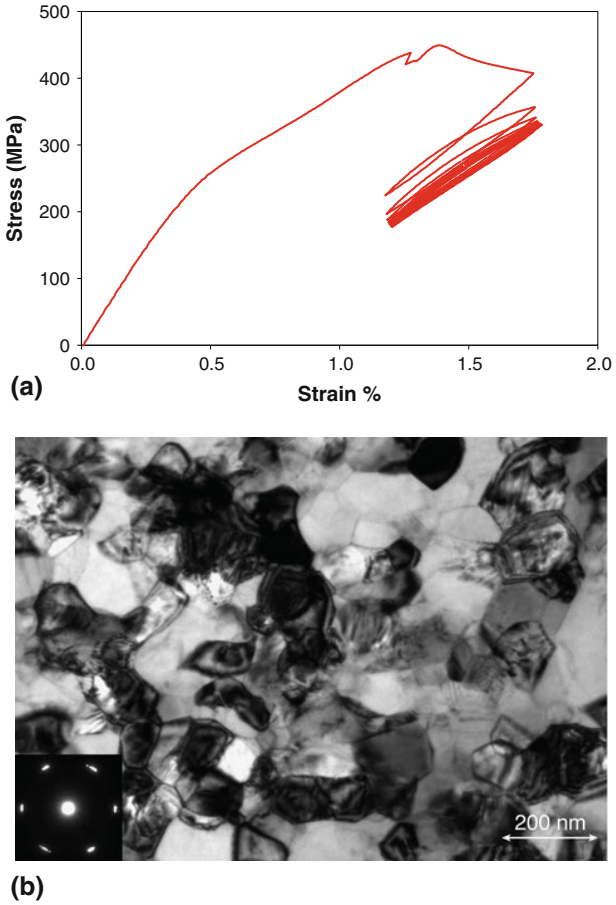

Fig. 4 (a) Stress-strain fatigue curves from stress-relieved superelastic $Ni_{50.8}Ti_{49.2}$ under conditions of 1.5% mean strain and strain amplitude of 0.25%. The cyclic curves are more stable than those shown in Fig. 3(a). (b) TEM microstructure after 10 cycles consists of 75 nm grains with dislocations and subgrains with no apparent retained martensite, similar to the non-fatigued microstructures, according to Ref 13

that similar microstructural effects were responsible for the observed changes in fatigue behavior investigations summarized above (Ref 10). Fatigue curves that correspond to the stress-relieved superelastic condition are shown in Fig. 4(a) (Ref 13). Note that this optimized processing (typical of Nitinol stent manufacturing) results in a more stabilized fatigue behavior with minimal softening and a relatively stable cyclic modulus. In contrast to the annealed microstructures, the stress-relieved and 10-cycle fatigued microstructure has an equiaxed grain size of approximately 75 nm with a $\{111\}_A$ texture (see inset diffraction pattern) as shown in Fig. 4(b). These austenitic grains contain dislocations and subgrains with no apparent retained martensite, similar to the non-fatigued microstructures.

Based on the TEM results discussed above, it is clear that processing plays a key role in the fatigue behavior of Nitinol. Testing under simulated in vivo conditions of process-optimized Nitinol is then required to gain insight into the fatigue behavior of biomedical devices. Tabanli et al. (Ref 14, 15) were the first to explore the effects of mean strain on the fatigue behavior of superelastic Nitinol hypotubing (A_f = 5 °C). Room temperature cycling was conducted at a constant strain amplitude of ~0.22%. The five mean strains ranged from 0.25 to 9.31% to capture the deformation of linear-elastic austenite, mixed phases of austenite and stress-induced martensite, and linear-elastic-deformed martensite. Based on these results, it was concluded that the Goodman constructions (Ref 16, 17) used for a linear-elastic constant-life diagrams are invalid for superelastic Nitinol. Tolomeo et al. (Ref 18) investigated the fatigue properties of sub-components that were cut from superelastic Nitinol stents, including laser machining, thermal expansion, and electropolishing. Testing was conducted to 10^6 cycles at 37 °C (A_f = 28 °C) for mean strains between 0.5 and 6% and strain amplitudes between 0.05 and 0.6%. There was an increase in fatigue life with mean strains between 1 and 5%, whereby the strain amplitude to fracture increased from 0.1 to 0.3%. Morgan et al. (Ref 19) observed similar behavior in superelastic wires (A_f = 12 °C) tested at 37 °C with mean strains between 2 and 6% and strain amplitudes between 0.5 and 3%. Furthermore, Pelton et al. (Ref 12, 20) investigated the fatigue behavior of Nitinol "diamond" test coupons cycled in bending to 10^7 cycles at 37 °C. Diamond-shaped specimens (see inset in Fig. 5) were laser machined from $Ni_{50.8}Ti_{49.2}$ tubing and were processed to achieve a target A_f of 30 °C, identical to many Nitinol stents. Fatigue results from five specimens per combination of mean

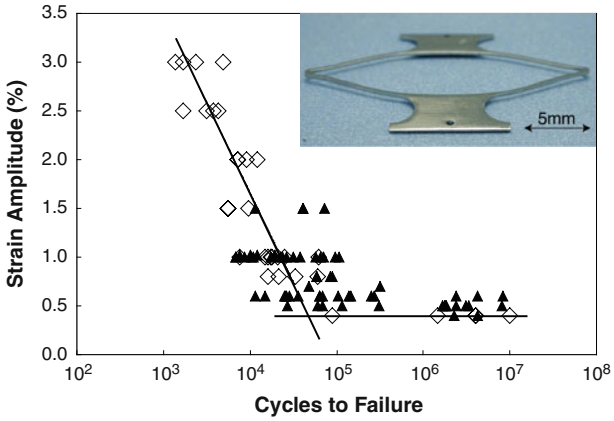

Fig. 5 Strain amplitude vs. fatigue data (strain-life) for conditions that led to fracture combinations of mean strain and strain amplitude are presented. The diagram can be separated into low-cycle (10^3 to 10^5 cycles) and high-cycle ($\geq 10^5$ cycles) regions. The fatigue strain limit at the high-cycle data is 0.4%, corresponding to the lowest strain amplitude where fractures were observed, according to Ref 12

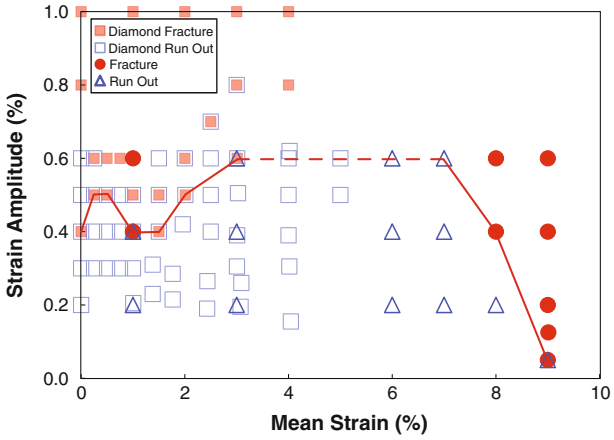

Fig. 6 Constant-life diagram from the diamond stent subcomponent fatigue testing where the various conditions of mean strain and strain amplitude are plotted. Also included are data from micro-dogbone specimens laser machined from $Ni_{50.8}Ti_{49.2}$ tubing with mean strains out to 9%. Conditions that survived the 10^7 cycle testing are shown as open squares, whereas cyclic conditions that led to fracture $<10^7$ cycles are represented with closed squares. Note that mean strain leads to increasing fatigue life in the 1.5-7% mean strain region, unlike conventional linear-elastic materials, according to Ref 12

strain (0-4%) and strain amplitudes (0.2-1.5%) are shown in Fig. 5. The data follow the expected trends of low-cycle fatigue behavior at the higher strain amplitudes and high-cycle fatigue behavior at the lower strain amplitudes. These fatigue-life data are re-plotted in a more illuminating manner in a constant-life diagram in Fig. 6. In addition to the "diamond" fatigue data, results from micro-dogbone specimens laser machined from $Ni_{50.8}Ti_{49.2}$ tubing with mean strains up to 9% are also included in this figure. The specimens that survived 10^7 cycles are shown as open symbols, whereas specimens that fractured are shown as solid symbols. A trend line was drawn to connect the lowest strain amplitude that resulted in fracture; this line therefore represents the 10^7-cycle life boundary. For mean strains between 1.5 and 3%, there is an increase in fatigue life from 0.4 to 0.6% strain amplitude. A dotted line at 0.6% strain amplitude is drawn between 3 and 7% mean strain to indicate that there are insufficient fracture data for complete analysis. Above 7% mean strain, which corresponds to the superelastic plateau length at 37 °C, however, the constant-life data exhibit a negative slope.

Mechanistically, it is clear that enhanced fatigue life between 1.5 and 7% mean strains is due to microstructural effects of stress-induced martensite. Hence, within this strain range, mean strain should be more accurately viewed as the volume fraction of stress-induced martensite. A few selected variants of stress-induced martensite (determined by the appropriate Taylor factors; Ref 21) reduce the internal strains due to the transformation. Collectively, these investigations demonstrate that the composite structure of stress-induced martensite plus austenite is able to accommodate a greater amount of strain amplitude, leading to longer fatigue lives, than either austenite or deformed martensite.

4. Summary

A review of the Nitinol fatigue literature demonstrates that cyclic transformations between austenite and martensite are more complicated than those that elastic (continuum) crystallographic theories predict. Thermal and mechanical cycling processess create plasticity, which may be due to the effects of moving martensite interfaces. Accumulation of the dislocations modifies transformational behavior, resulting in changes in transformation temperatures, strain (under stress-control) and stress (under strain-control). Processing has a major effect on fatigue properties, whereby optimized thermomechanically treated microstructures yield more stable (and predictable) behavior than annealed microstructures.

Acknowledgments

The author acknowledges the stimulating conversations on Nitinol fatigue with B. Berg, T. Duerig, A. Mehta, M.R. Mitchell, R.O. Ritchie, and S.W. Robertson.

References

1. T.W. Duerig, K.N. Melton, D. Stöckel, and C.M. Wayman, *Engineering Aspects of Shape Memory Alloys*, Butterworth-Heinemann, London, 1990
2. D. Stöckel, A.R. Pelton, and T. Duerig, Self-Expanding Nitinol Stents: Material and Design Considerations, *Eur. Radiol.*, 2004, **14**, p 292–301
3. K. Bhattacharya, *Microstructure of Martensite*, Oxford University Press, Oxford, 2003
4. K. Otsuka and X. Ren, Physical Metallurgy of Ti-Ni-Based Shape Memory Alloys, *Prog. Mater. Sci.*, 2005, **50**, p 511–678
5. A.R. Pelton, G.H. Huang, P. Moine, and R. Sinclair, Transformation-Induced Dislocations in Ti-Ni, Unpublished 2010
6. G. Airoldi, B. Rivolta, and C. Turco, Heats of Formation as a Function of Thermal Cycling in NiTi Alloys, *International Conference on Martensitic Transformations*, Tokyo, 1986, p 691–696
7. S. Miyazaki, Y. Igo, and K. Otsuka, Effect of Thermal Cycling on the Transformation Temperatures of Ti-Ni Alloys, *Acta Metall.*, 1986, **34**, p 2045–2051
8. D.M. Norfleet, P.M. Sarosi, S. Manchiraju, M.F.X. Wagner, M.D. Uchic, P.M. Anderson, and M.J. Mills, Transformation-Induced Plasticity During Pseudoelastic Deformation in Ni-Ti Microcrystals, *Acta Mater.*, 2009, **57**, p 3549–3561

9. T. Simon, A. Krôger, C. Somsen, A. Dlouhy, and G. Eggeler, On the Multiplication of Dislocations During Martensitic Transformations in NiTi Shape Memory Alloys, *Acta Mater.*, 2009, **58**, p 1850–1860
10. K.N. Melton and O. Mercier, Fatigue of NiTi Thermoelastic Martensites, *Acta Metall.*, 1979, **27**, p 137–144
11. T.W. Duerig, D.E. Tolomeo, and M. Wholey, An Overview of Superelastic Stent Design, *Minim. Invasive Ther. Allied Technol.*, 2000, **9**, p 235–246
12. A.R. Pelton, V. Schroeder, M.R. Mitchell, X.-Y. Gong, M. Barney, and S.W. Robertson, Fatigue and Durability of Nitinol Stents, *J. Mech. Behav. Biomed. Mater.*, 2008, **1**, p 153–164
13. A.R. Pelton and M.R. Mitchell, Microstructural Effects of Mechanically Cycled Nitinol, unpublished 2006
14. R.M. Tabanli, N.K. Simha, and B.T. Berg, Mean Stress Effects on Fatigue of NiTi, *Mater. Sci. Eng. A*, 1999, **273–275**, p 644–648
15. R.M. Tabanli, N.K. Simha, and B.T. Berg, Mean Strain Effects on the Fatigue Properties of Superelastic NiTi, *Metall. Mater. Trans. A*, 2001, **32A**, p 1866–1869
16. M.R. Mitchell, Fundamentals of Modern Fatigue Analysis for Design, *ASM Handbook*, Fatigue and Fracture, Materials Park, OH, 1996, p 227–262
17. S. Suresh, *Fatigue of Materials*, Cambridge University Press, 1998
18. D. Tolomeo, S. Davidson, and M. Santinoranout, Cyclic Properties of Superelastic Nitinol: Design Implications, *SMST-2000: Proceedings of the International Conference on Shape Memory and Superelastic Technologies*, S.M. Russell and A.R. Pelton, Ed. (Pacific Grove, CA), International Organization on SMST, 2000, p 409–417
19. N.B. Morgan, J. Painter, and A. Moffat, Mean Strain Effects and Microstructural Observations During In Vitro Fatigue Testing of NiTi, *SMST-2003: Proceedings of the International Conference on Shape Memory and Superelastic Technologies*, A.R. Pelton and T.W. Duerig, Ed. (Pacific Grove, CA), International Organization on SMST, 2003, p 303–310
20. A.R. Pelton, X.-Y. Gong, and T. Duerig, Fatigue Testing of Diamond-Shaped Specimens, *SMST-2003: Proceedings of the International Conference on Shape Memory and Superelastic Technologies*, A. Pelton, and T. Duerig, Ed. (Pacific Grove, CA), International Organization on SMST, 2003, p 293–302
21. N. Ono and A. Sato, Plastic Deformation Governed by the Stress Induced Martensitic Transformation in Polycrystals, *Trans. Jpn. Inst. Met.*, 1988, **29**, p 267–273